



Published in final edited form as:

Magn Reson Med. 2011 April ; 65(4): 1097–1102. doi:10.1002/mrm.22687.

Respiratory bellows revisited for motion compensation: preliminary experience for cardiovascular MR

Claudio Santelli^{1,2}, Reza Nezafat², Beth Goddu², Warren J. Manning^{2,3}, Jouke Smink⁴, Sebastian Kozerke¹, and Dana C. Peters²

¹Swiss Federal Institute of Technology, Zurich, Switzerland ²Beth Israel Deaconess Medical Center, Department of Medicine (Cardiovascular Division) ³Beth Israel Deaconess Medical Center, Department of Radiology, Best, NL ⁴Philips Healthcare, Best, NL

Abstract

For many cardiac MR applications, respiratory bellows-gating is attractive because it is widely available and not disruptive to or dependent on imaging. However, its use is uncommon in cardiac MR, because its accuracy has not been fully studied. Here, in 10 healthy subjects, the bellows and respiratory navigator (NAV) the displacement of the diaphragm and heart were simultaneously monitored, during single-shot imaging. Furthermore, bellows-gated and NAV-gated coronary MRI were compared, using a retrospective reconstruction at identical efficiency. There was a strong linear relationship for both the NAV and the abdominal bellows with the diaphragm ($R=0.90\pm 0.05$ bellows, $R=0.98\pm 0.01$ NAV, $p<0.001$) and the heart ($R=0.89\pm 0.06$ bellows, $R=0.96\pm 0.02$ NAV, $p=0.004$); thoracic bellows correlated less strongly. The image quality of bellows-gated coronary MRI was similar to NAV-gated, and superior to no-gating ($p<0.01$). In conclusion, bellows provides a respiratory monitor which is highly correlated with the NAV, and suitable for respiratory-compensation in selected cardiac MR applications.

Introduction

Respiratory and cardiac motion compensation are essential in cardiovascular magnetic resonance (CMR) to suppress motion artifacts. ECG-gating, while reducing cardiac motion, increases the problem of respiratory motion, by increasing scan time. In CMR, respiratory motion must be minimized, and this is performed mainly using a breath hold, or free-breathing navigator-gated (NAV) strategies (1,2).

Sustained breath-holding limits scan time to about 20 seconds. Furthermore, there is variability between each breath-hold (3,4). NAV-gating typically monitors the diaphragmatic displacement, which correlates with the respiratory motion of the heart, albeit with a patient-dependent factor (1). The NAV pulse excites the right hemi-diaphragm tissue to track the lung-liver interface. The location of the interface provides a criterion to accept or reject the corresponding data segment. The NAV excitation pulse itself requires about 30 ms, and is usually applied once, about 50 ms before acquisition.

Although developed early (5), respiratory bellows is no longer commonly used and its accuracy has not been fully evaluated for CMR. In an early study comparing bellows-gating to NAV-gating for coronary MRI, NAV gating had a small benefit in image quality; but,

bellows had a higher gating efficiency (6). Studies have disclosed a very strong correlation between bellows and diaphragmatic motion (7-9). Bellows gating has attractive qualities. It provides a continuous signal which does not disrupt imaging, in stark contrast to NAV-gating and even most self-gating methods. This may prove useful, e.g. for cine imaging or to restrict imaging based on criteria derived from multiple time points during the acquisition. The bellows signal is independent of field strength (3T or 7T), while this is not true for the NAV (10), especially pencil beam excitations. Finally, the bellows-signal is independent of any preparation pulses that might affect the MR signal, unlike the NAV that, for example, must be modified for late gadolinium enhancement sequences (11), with resulting artifacts (12).

The goal of this study was to quantitatively evaluate respiratory bellows to determine its correlation with the NAV for monitoring motion of the heart, and to preliminarily investigate the application of bellows-gating for coronary MRI.

Materials and Methods

Ten adult healthy subjects (5 female, age 20 ± 2 years) were studied on a 1.5T Philips Achieva (Philips Healthcare Systems, Best, NL). All subjects provided written informed consent and the study was approved by our Institutional Review Board.

Imaging and Analysis

2D single-shot imaging was performed during free-breathing using balanced steady state free precession (SSFP), 32×32 cm FOV, providing $3 \times 3 \times 8$ mm³ spatial resolution before zero-filing within 200 ms acquisition window, using TR/TE/ $\theta=2.2$ ms/1.1ms/60°. MR imaging was performed with a single-shot acquisition ECG-gated to mid-diastole. Coronal images capturing the dome of the diaphragm and the heart were obtained. The diaphragm and heart displacements were monitored using regions of interest (ROIs) (Figure 1) and cross-correlation methods in the superior-inferior (SI) direction, with quarter-pixel accuracy, using interpolation. The SI displacement of each image, x_i , was measured. The average variation in heart SI displacement for a particular set of N images, selected using a particular NAV or bellows criteria, was calculated as

$$\bar{x} = \frac{\sum |x_i - x_0|}{N}, \quad (1)$$

where x_0 is the average heart SI position over the N selected images.

Prior to each image, NAV-monitoring of the right hemi-diaphragm was obtained, without gating or tracking. The respiratory bellows signal was continuously recorded (500Hz) during acquisition of 100 frames. In the bellows file, the time of data acquisition was marked for each frame. The bellows signal corresponding to each image was extracted, by obtaining the bellows signal mostly closely coinciding with the collection of the center of k-space. Similarly, a bellows signal corresponding to the time of NAV-monitoring was extracted, 35 ms prior to image acquisition. No time shifting was applied to the bellows data. In all subjects, the bellows was placed on the abdomen, and then the data was reacquired with the bellows placed on the chest wall, at the sternum (20-30 minutes later) –the thoracic bellows. The bellows was commercially provided (Philips Healthcare, Best NL), consisting of a pressure-sensing pillow, which was semi-tightly wedged between the subject, and a hard surface (e.g. the ECG sensor box), following our standard clinical subject preparation.

Coronary MRI—Coronary MRI was performed during free-breathing, with the full 3D volume acquired 5 times (in 3/10 subjects, only twice), and NAV and bellows-monitoring, but no slice-tracking. The right coronary artery was imaged using a 3D targeted approach. Acquisition parameters were: 3D gradient echo, TR/TE/ θ = 5.5ms/1.8ms/25°, partial echo, 16 views per heart-beat with centric acquisition order, 256 Nx × 256 Ny × 13 Nz matrix, 27 cm FOV, 3 mm slice thickness, T2prep and fat-saturation, ECG-gating to mid-diastole. Images were reconstructed retrospectively off-line using Matlab (Matlab v. 7.1, Mathworks, Natick, MA). The data was reconstructed using 1) no respiratory gating (using a single acquisition without averaging), 2) a 5 mm NAV window (7mm if only 2 acquired volumes), and 3) using bellows-gating criteria at identical scan efficiency. Because of the retrospective acquisition, the best data from outside this window was used if necessary. Assuming 50% efficiency, even after 5 acquisitions, on average ~2% of the k-space will be outside the acceptance range.

For coronary MRI, the source images reconstructed by bellows-gating, NAV-gating and free-breathing were graded on a 1-4 point scale by a blinded experienced reader in randomized order (1 = non-diagnostic, 2 = significant blurring and ghosting, 3 = some blurring and ghosting, 4 = no apparent blurring and ghosting). Coronary artery sharpness was also graded on a 4-point scale (4 = excellent). The right coronary artery lengths were measured using the SoapBubble tool(13), and reformatted for visualization.

Statistics

All data are presented as mean \pm standard deviation. The R-values and mean deviations of the heart were compared using the student's t-test. The subjective image quality scores were compared using the Wilcoxon signed-rank test. A $p < 0.05$ was considered significant.

Results

Data from 10 subjects was successfully acquired to study the relationship of abdominal bellows to NAV and heart displacements; for the chest wall, data from 9 subjects was available. The average respiratory period was 3.8 ± 0.6 seconds/breath. The average diaphragmatic excursion (peak to trough) was 12 ± 4 mm. A representative result in one subject for abdomen bellows is presented in Figure 2. Figure 2A plots bellows and the NAV vs. time, while Figure 2B-D demonstrates the strong correlation of bellows with NAV, diaphragm, and heart. Figure 2B illustrates how the selection of windows for bellows and NAV is performed: the choice of a 5mm NAV window sets an efficiency that can guide choice of a corresponding bellows window, which is strongly overlapping. Figure 2E-F show the excellent correlation of the NAV with the heart and the diaphragm, with bellows also strongly correlated. Figure 2G-H presents the relationship between NAV and thoracic bellows, for the same subject. Note the reduced correlation, and greater phase offset. Table 1 presents summary data for all subjects. Note that the R value was greater for NAV vs. the heart than for abdominal bellows vs. the heart ($p = 0.004$). Figure 2I shows a patient (selected because of their large diaphragmatic excursion and unusual breathing pattern, and not included in quantitative analysis) undergoing coronary MRI, comparing bellows and NAV for a segment of the acquisition. In this comparison, in which the patient is exhibiting a long respiratory period with significant respiratory drift (a less common but well-known and challenging respiratory pattern), and a large diaphragmatic excursion, the bellows is less strongly correlated, primarily matching the NAV only in respiratory phase.

Figure 3 plots the average variation in cardiac SI displacement (Equation 1) resulting from each NAV-gating window, and each corresponding bellows window; the variation ideally is zero. The NAV and bellows perform similarly for windows of 7mm or greater, with NAV

performing better at 3-5mm, although this was not significant ($p=0.06$ at 3mm). The NAV was better than free-breathing (i.e. 15mm window) for all NAV windows less than 13 mm, as was the bellows. The thoracic bellows performed worse than the abdominal bellows, as evidenced by a lower correlation (R value) to cardiac displacement (0.89 vs. 0.81, $p=0.02$), and a higher average deviation of the heart ($p<0.01$).

Figure 4 shows a comparison of no-gating, bellows-gating and NAV-gating for coronary MRI, using retrospective bellows and NAV-gated reconstructions with identical efficiency ($62\pm 12\%$, equivalent to a 5 mm window). The average score for motion blurring and ghosting from the 10 subjects was 3.4 ± 0.8 , 3.3 ± 0.7 and 2.4 ± 0.7 for NAV-, bellows- and no-gating, respectively ($p<0.01$, NAV vs. no-gating; $p=NS$, NAV vs. bellows). For coronary vessel sharpness, the average scores were 3.0 ± 0.9 , 3.2 ± 0.6 , and 2.0 ± 0.5 for NAV-, bellows- and no-gating respectively ($p<0.01$, NAV vs. no-gating; $p=NS$, NAV vs. bellows). Coronary artery lengths were 47 ± 11 mm, 44 ± 9 mm, and 35 ± 6 mm for NAV-, bellows- and no-gating respectively ($p<0.01$, NAV vs. no-gating; $p=NS$, NAV vs. bellows).

Discussion

The main finding of this study of healthy subjects is a strong linear relationship between abdominal bellows and the NAV ($R=0.91\pm 0.05$), the diaphragm ($R=0.90\pm 0.05$) and the heart ($R=0.89\pm 0.06$), with thoracic bellows less strongly correlated. The bellows signal provides similar respiratory compensation as the NAV for all NAV acceptance windows, although the NAV provided a non-significant reduction in heart displacement for windows less than 7mm. The coronary image quality was not different, comparing bellows and NAV-gating, but there was reduced quality with no respiratory compensation (2.7 vs. 3.7, $p<0.01$). A larger study might reveal differences between NAV and bellows for high resolution coronary scans (3.7 vs. 3.4, $p=0.16$ in our study). However for many applications, such as higher resolution 3D late gadolinium enhancement studies, bellows may be accurate enough to replace the NAV.

Possible reasons for the poorer correlation between thoracic bellows and NAV are phase offsets in the periodic signals between the thoracic bellows and the diaphragmatic motion(14), reduced range of motion in chest wall compared to the abdomen, or possibly, a changed and more challenging breathing pattern later in the scan session—the thoracic bellows data were always acquired later in the exam.

Further work is needed to determine the optimal manner for employing bellows for CMR. This includes more precisely determining the optimal location for bellows placement, identifying subjects who are good/poor candidates for bellows gating including gender differences, refining bellows-gating windows, determining the limits on its accuracy, and exploiting its unique feature of continuous respiratory information, some of which are addressed to some degree in this study. Bellows is limited in that it provides only a relative measure of respiration, the percentage of the maximal respiratory amplitude, but cannot provide absolute displacements as the NAV can provide for diaphragmatic motion. A prescan, in which real-time imaging, ROI-tracking, and bellows-monitoring were performed, would allow calculation of the heart SI motion vs. bellows amplitude (e.g. Figure 2D), but may not be robust to respiratory drift, and its automation is challenging.

Finally, the use of bellows-gating for other applications such as cardiac cine, where the NAV is possible but challenging (15), high field imaging, and late gadolinium enhancement imaging might provide advantages.

Non-linear bellows signal

The bellows signal, although well correlated with the NAV under regular breathing patterns, will not vary linearly with diaphragmatic or heart motion under some circumstances. Therefore, bellows-gating may not be compatible with slice-tracking, since the bellows is less quantitative. Furthermore, its ability to track the heart during a shifting breathing pattern may be poor, due to possible rescaling of the bellows signal, or other non-linearities, as shown in Figure 2I. (16). Further work is needed to study the optimal method for choosing a bellows-gating window.

Limitations

The spatial resolution of the single shot images was low, and this may have affected the correlations between NAV or bellows with the heart and diaphragmatic position; future studies should employ higher readout (superior-inferior) resolution. Our scanner is equipped with a pillow bellows, but it is likely to perform similarly to a belt bellows system. The study was small, and only included healthy young subjects who may not be representative of patients in their breathing patterns. This may have caused unrepresentative higher quality of the un-gated coronary MRI (Figure 4). A patient study including subjects with greater diaphragmatic excursions and drifting breathing patterns is warranted to further clarify the strengths and weaknesses of bellows-gating. In some subjects, strong hysteresis effects (17,18) might reduce the linearity between the heart and both the NAV and bellows signals.

Conclusion

In healthy subjects, the abdominal bellows provides a signal that is highly correlated to superior-inferior motion of the diaphragm and heart, and to the NAV signal. The thoracic bellows is less strongly correlated than the abdominal bellows. For coronary MRI, bellows-gating provided images of similar quality to NAV-gating in a small study. Bellows provides a monitor suitable for respiratory-compensation in selected cardiac MR applications.

Acknowledgments

Supported in part by grants from the American Heart Association (AHA SDG 0530061N) and the National Institutes of Health (NIBIB K01 EB004434-01A1, NHLBI 1R21HL098573-01)

Bibliography

1. Wang Y, Riederer SJ, Ehman RL. Respiratory motion of the heart: kinematics and the implications for the spatial resolution in coronary imaging. *Magn Reson Med*. 1995; 33:713–719. [PubMed: 7596276]
2. Wang Y, Grimm RC, Rossman PJ, Debbins JP, Riederer SJ, Ehman RL. 3D coronary MR angiography in multiple breath-holds using a respiratory feedback monitor. *Magn Reson Med*. 1995; 34:11–16. [PubMed: 7674888]
3. Fischer RW, Botnar RM, Nehrke K, Boesiger P, Manning WJ, Peters DC. Analysis of residual coronary artery motion for breath hold and navigator approaches using real-time coronary MRI. *Magn Reson Med*. 2006; 55:612–618. [PubMed: 16453319]
4. Holland AE, Goldfarb JW, Edelman RR. Diaphragmatic and cardiac motion during suspended breathing: preliminary experience and implications for breath-hold MR imaging. *Radiology*. 1998; 209:483–489. [PubMed: 9807578]
5. Ehman RL, McNamara MT, Pallack M, Hricak H, Higgins CB. Magnetic resonance imaging with respiratory gating: techniques and advantages. *AJR Am J Roentgenol*. 1984; 143:1175–1182. [PubMed: 6333787]

6. McConnell MV, Khasgiwala VC, Savord BJ, Chen MH, Chuang ML, Edelman RR, Manning WJ. Comparison of respiratory suppression methods and navigator locations for MR coronary angiography. *AJR Am J Roentgenol.* 1997; 168:1369–1375. [PubMed: 9129447]
7. Martinez-Moller A, Zikic D, Botnar RM, Bundschuh RA, Howe W, Ziegler SI, Navab N, Schwaiger M, Nekolla SG. Dual cardiac-respiratory gated PET: implementation and results from a feasibility study. *Eur J Nucl Med Mol Imaging.* 2007; 34:1447–1454. [PubMed: 17318548]
8. Spincemaille, P.; Nguyen, TD.; Prince, MR.; Wang, Y. Quantitative study of motion detection performance of center of k-space measurements. *International Society of Magnetic Resonance in Medicine; Berlin, Germany: 2007.* p. 1826
9. Madore B, Farneback G, Westin CF, Duran-Mendicuti A. A new strategy for respiration compensation, applied toward 3D free-breathing cardiac MRI. *Magn Reson Imaging.* 2006; 24:727–737. [PubMed: 16824968]
10. Stuber M, Botnar RM, Fischer SE, Lamerichs R, Smink J, Harvey P, Manning WJ. Preliminary report on in vivo coronary MRA at 3 Tesla in humans. *Magn Reson Med.* 2002; 48:425–429. [PubMed: 12210906]
11. Spuentrup E, Buecker A, Karassimos E, Gunther RW, Stuber M. Navigator-gated and real-time motion corrected free-breathing MR Imaging of myocardial late enhancement. *Rofo.* 2002; 174:562–567. [PubMed: 11997854]
12. Peters DC, Wylie JV, Hauser TH, Kissinger KV, Botnar RM, Essebag V, Josephson ME, Manning WJ. Detection of pulmonary vein and left atrial scar after catheter ablation with three-dimensional navigator-gated delayed enhancement MR imaging: initial experience. *Radiology.* 2007; 243:690–695. [PubMed: 17517928]
13. Etienne A, Botnar RM, Van Muiswinkel AM, Boesiger P, Manning WJ, Stuber M. “Soap-Bubble” visualization and quantitative analysis of 3D coronary magnetic resonance angiograms. *Magn Reson Med.* 2002; 48:658–666. [PubMed: 12353283]
14. Pengelly LD, Tarshis AM, Rebuck AS. Contribution of rib cage and abdomen-diaphragm to tidal volume during CO2 rebreathing. *J Appl Physiol.* 1979; 46:709–715. [PubMed: 156712]
15. Peters DC, Nezafat R, Eggers H, Stehning C, Manning WJ. 2D free-breathing dual navigator-gated cardiac function validated against the 2D breath-hold acquisition. *J Magn Reson Imaging.* 2008; 28:773–777. [PubMed: 18777547]
16. Danias PG, McConnell MV, Khasgiwala VC, Chuang ML, Edelman RR, Manning WJ. Prospective navigator correction of image position for coronary MR angiography. *Radiology.* 1997; 203:733–736. [PubMed: 9169696]
17. Keegan J, Gatehouse P, Yang GZ, Firmin D. Coronary artery motion with the respiratory cycle during breath-holding and free-breathing: implications for slice-followed coronary artery imaging. *Magn Reson Med.* 2002; 47:476–481. [PubMed: 11870834]
18. Nehrke K, Bornert P, Manke D, Bock JC. Free-breathing cardiac MR imaging: study of implications of respiratory motion--initial results. *Radiology.* 2001; 220:810–815. [PubMed: 11526286]

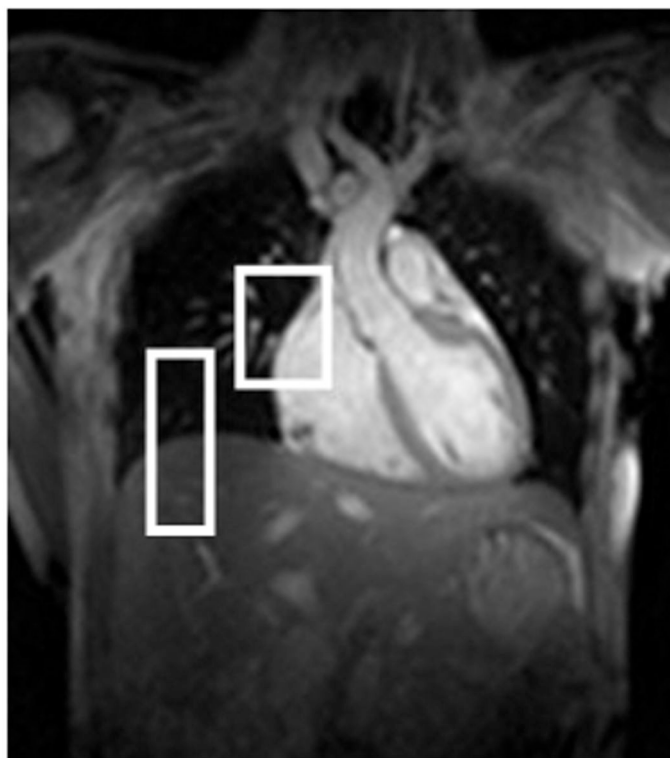


Figure 1. Representative image from the single-shot images, showing the ROIs used for tracking the SI motion of the diaphragm and the heart.

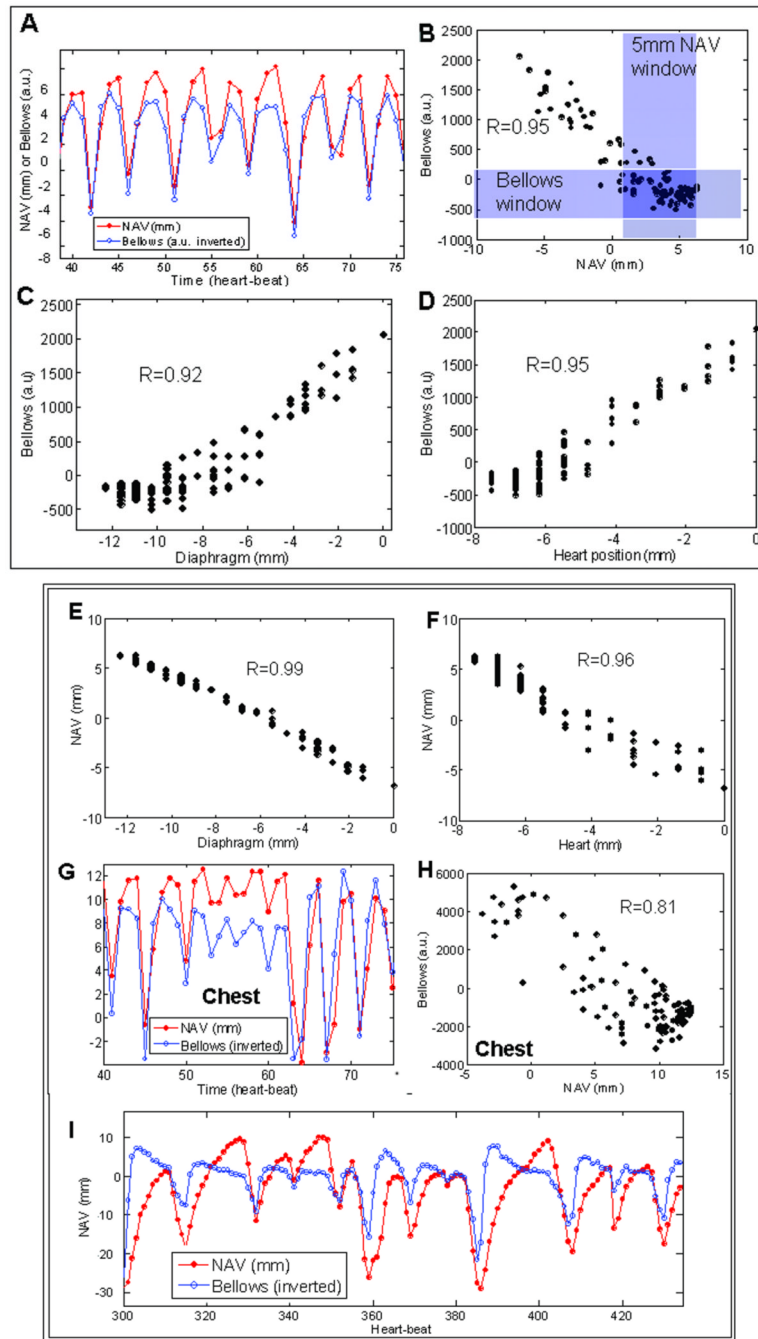


Figure 2.

Results from a single representative subject comparing the NAV, bellows, diaphragm and heart. A-F) Abdominal bellows. A). The NAV and bellows tracings are overlaid, revealing an approximately synchronous relationship. B) A linear relationship was found between the bellows and NAV data, with potential gating windows indicated (5mm NAV window, and a Bellows window with identical efficiency). C) Bellows vs. diaphragmatic SI position, and D) bellows vs. heart. All tracings indicate the utility of bellows a surrogate for the NAV. E) NAV vs. diaphragm, F) NAV vs. heart. G-H) Thoracic bellows. G) Bellows and NAV vs. time, with bellows placed on the chest wall (thoracic bellows signal). H) Bellows vs. NAV.

Note poorer correlation with thoracic bellows, and the appearance of a phase-offset (NAV and bellows are not in sync). I) Patient study, showing an example of respiratory drift. For this respiratory pattern, the bellows is less well correlated with the NAV.

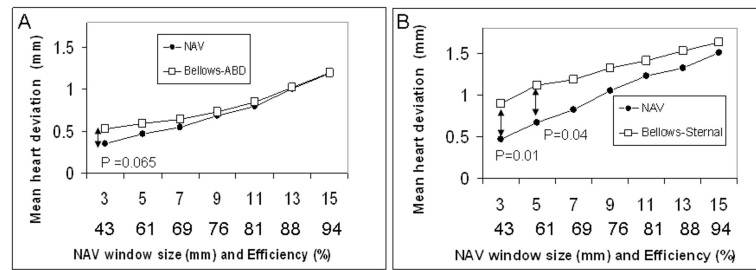


Figure 3.

A) The average SI displacement of the heart, using NAV and abdominal bellows at different gating efficiencies or NAV acceptance windows. B) Thoracic bellows. The thoracic bellows data was collected about 30 minutes after the abdominal bellows data, and breathing motion appears to be greater (1.5 mm vs. 1.2 mm of variability) in the later data set.

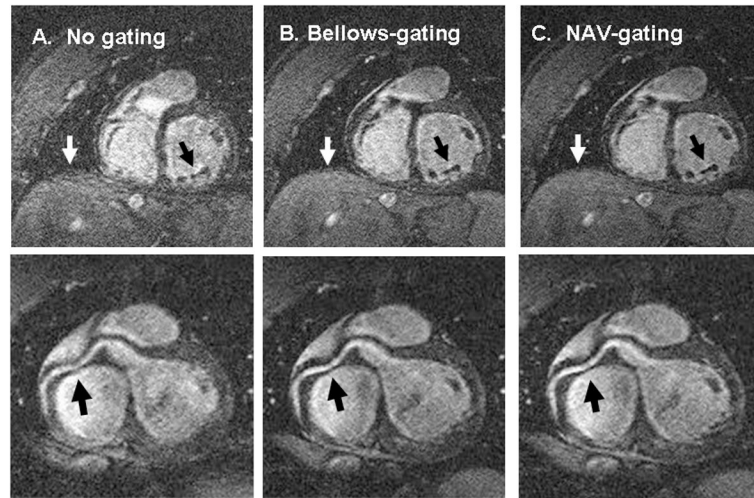


Figure 4. Coronal MRI of the right coronary artery with A) no gating, B) bellows-gating and with C) NAV-gating, using retrospective reconstruction. Upper row shows slices, lower rows show a maximum intensity projection (MIP). Clear improvement in image quality using NAV- and bellows-gating compared to no gating is evident in the sharpness of the papillary muscles, diaphragm, and the coronary artery (arrows).

Table 1
Relationship between bellows, NAV, diaphragm and heart

	R_{Heart}	\bar{x} (Mean heart deviation) *	R_{NAV}	$R_{\text{Diaphragm}}$
NAV	0.96±0.02	0.47±0.16	1	0.98±0.01 ^{††}
Bellows _{Abd}	0.89±0.06 [†]	0.59±0.19	0.91±0.05	0.90±0.05
Bellows _{Strn}	0.81±0.08 [‡]	1.1±0.32 ^{***}	0.83±0.08	0.82±0.08

[†] p=0.004 vs. NAV.

[‡] p=0.02 vs. abdomen bellows.

^{***} p=0.004 thoracic vs. abdomen bellows.

^{††} p<0.001 vs. abdominal bellows.

* For a 5 mm NAV-window.